Synthetic Metals 246 (2018) 39–44

Contents lists available at ScienceDirect

Synthetic Metals

journal homepage: www.elsevier.com/locate/synmet

Photophysical, spectroscopic properties and electronic structure of BND: Experiment and theory

Emine Babur Sas[a,*], Mustafa Kurban[a,*], Bayram Gündüz[b,*], Mustafa Kurt[c]

[a] Department of Electronics and Automation, Ahi Evran University, 40100, Kırşehir, Turkey
[b] Department of Science Education, Faculty of Education, Muş Alparslan University, 49250, Muş, Turkey
[c] Department of Physics, Ahi Evran University, 40100, Kırşehir, Turkey

ARTICLE INFO

Keywords:
BND
Oxadiazoles
Optical parameters
Optical band gap
DFT

ABSTRACT

The electronic structure, photophysical and spectroscopic properties of 2,5-Bis(1-naphthyl)-1,3,4-oxadiazole (BND) have been researched based on different solvent environments. The refractive index (n) is calculated using the semi-empirical relations based on measured energy gap (E_g) data. The lowest harmonic frequencies, Mulliken atomic charges, dipole moments, HOMO and LUMO energies were investigated using density functional theory (DFT). Moreover, ultraviolet-visible (UV–vis), energy gaps and radial distribution functions (RDFs) have been carried out using experiment and theory with B3LYP and CAM-B3LYP functionals. We also obtained the absorbance band edge and mass extinction coefficient of the BND solutions for dichloromethane (DCM) and chloroform. In addition, we investigated the optical and electrical conductance of the BND for related solvents. The HOMO and LUMO energy levels of the BND molecule in different solvent environments range from -2.17 to 2.21 eV and from -6.10 to -6.22 eV, indicating that the BND molecule will function well as electron transport materials in OLED applications. From obtained results, BND material has suitable optoelectronic parameters for the construction of functional materials, especially OLEDs.

1. Introduction

Organic light-emitting diodes (OLEDs) have a wide range of applications such as optical, electronic, optoelectronic and photonic technology [1–7]. Especially, OLEDs have widely been used in the panel displays and solid-state lightings [8,9]. To obtain the practical application of OLEDs, achieving highly efficient OLEDs with a simple structure is always essential [10–13]. In this regard, the designed materials for OLEDs require special properties such as proper HOMO and LUMO energy levels [14], high luminescence efficiency [15], balanced charge-carrier mobility [16], and good stability [17]. Among OLEDs, oxadiazoles are the most widely used in areas in pharmaceutical chemistry and material science due to their remarkable optoelectronic properties [18]. In the literature, a series of available oxadiazoles and its derivatives were studied due to their high potential of electron-transporting from evaluating electron mobility, facile injection, good chemical and thermal stability [19–23]. Especially, compounds bearing the 1,3,4-oxadiazole core, mainly the 2,5-disubstituted ones, have been continuously developed due to their desirable optical and electronic properties that make them suitable candidates for the preparation of OLEDs [24–26]. Among these compounds, 2.5-bis(1-naphthyl)-1,3,4-oxadiazole (BND) is a very important material which exhibits the highest value of electron mobility than that of the other derivatives [27]. In this regard, various studies have been conducted on BND organic molecule. For example, the anthracene derivatives of BND have considerable potential as multifunctional layers and an electron transport layers in OLED [28].

Structure of organic compounds has a significant impact on the properties of materials, especially in the solvent environment [29–32]. A solute-solvent morphology plays a crucial role in the performance of devices based on those materials because the solvent environments induce the significant changes in the physical and chemical properties of material [33]. To our knowledge, there is no any information on the photophysical, electronic structure and spectroscopic properties of BND organic material in different solvent environments. From this viewpoint, the major aim of the present study is to probe the features mentioned above of the BND organic material in different solvent environments using experimental technique and density functional theory (DFT) approach in the literature.

This article is organized as follows: we theoretically analyzed the lowest harmonic frequencies with positive value to gain insight into the most stable optimized structure. Then, Mulliken atomic charges, dipole

* Corresponding authors.
E-mail addresses: baburemine@gmail.com (E.B. Sas), mkurbanphys@gmail.com (M. Kurban), bgunduz83@hotmail.com (B. Gündüz).

https://doi.org/10.1016/j.synthmet.2018.09.013
Received 16 May 2018; Received in revised form 23 September 2018; Accepted 24 September 2018
Available online 05 October 2018

moments, the highest occupied molecular orbital (HOMO), the lowest unoccupied molecular orbital (LUMO) and the frontier molecular orbital energy gap (HOMO–LUMO difference in energy gap, E_g) were investigated using DFT approach. These properties were controlled with different solvents such as dichloromethane (DCM), dichloroethane (DCE), dimethyl sulfoxide (DMS), acetonitrile and chloroform. Calculated E_g values obtained from B3LYP and CAM-B3LYP functionals were compared with the measured E_g values for different solvents. The calculated ultraviolet-visible (UV–vis) spectra obtained from time-dependent (TD)-DFT method have been compared with the measured results. In addition, the photoluminescence (PL) spectra have been calculated in different solvents based on TD-DFT calculations. The optical refractive index (n) is calculated using the semi-empirical relations based on measured energy gap (E_g) data. Later, the effects of the solvents on the mass extinction coefficient, $(\alpha h\vartheta)^2$ curves based on the photon energy (E), density of state (DOS) spectrum obtained Mulliken population analysis, optical conductance (σ_{opt}) and electrical conductance (σ_{elect}) and the radial distribution functions (RDFs) were investigated. Finally, we discussed these parameters based on different solvent environments in detail.

2. Experimental details

DCM and chloroform solvents, and 2,5-bis(1-naphthyl)-1,3,4-oxadiazole (BND), whose synonym is 2,5-di(naphthalen-1-yl)-1,3,4-oxadiazole were purchased from a chemical company (Sigma-Aldrich, USA). The BND material was adjusted for 0.35 *mM* molarity and was separately dissolved in 20 mL volume of the DCM and chloroform solvents. Thence, we obtained the BND solutions for different solvents. Then, we took the measurements of the UV-spectra with a UV-1800 Spectrophotometer (Shimadzu model, Japan) at room temperature.

3. Computational details

Photophysical, electronic structure and spectroscopic properties of BND organic material have been searched using DFT [34] with B3LYP functional [35–37] and 6–311 G (d, p) basis set. CAM-B3LYP [38] functional were also tested for accuracy and efficiency of the calculations because B3LYP actually underestimates excited-state energies [39–41]. Even so, the results obtained from B3LYP were also compared with CAM-B3LYP in this study because, especially for some molecular systems, excited state energy obtained from B3LYP functional gives better results [14,42]. GAUSSIAN09 program package is used in the calculations [43]. To obtain the most stable structure with minimum total energy without imposing any symmetrical constraints, various spin multiplicities were performed and found that spin singlet gives the most stable structure which assumed as the global minimum case. The most stable structure is taken as the local minima on potential energy surface with positive vibration frequencies. Using optimized geometry, the maximum wavelengths are obtained from TD-DFT method compared with the measured ones of BND organic molecule.

4. Results and discussion

4.1. Structural analysis

Optimized geometry of BND organic molecule with atom numbering calculated by B3LYP/6-311-G (d, p) is indicated in Fig. 1. From DFT calculations, the positive vibrational spectra were found that the optimized geometry is located at stationary point on the potential energy surface. The lowest vibrational harmonic frequencies of BND molecule are found to be 12.6, 12.7, 14.6, 14.4 and 13.9 cm^{-1} in DCM, DCE, DMS, acetonitrile and chloroform solvents, respectively. From this results, one can conclude that the compound in DCM is more stable than that of chloroform. Form the geometrical optimization results, the structure with minimum total energy is the C_1 form.

4.2. Absorption and emission spectra properties

The optical properties of the BND material for different solvents were investigated using the data of the UV spectra with experimental and theoretical techniques. Fig. 2a indicates the experimental absorbance (Abs) and theoretical molar absorptivity spectra vs. wavelength (λ) of the BND material for various solvents. As seen in Fig. 2a, the BND material exhibits the maximum peaks of the absorbance and molar absorptivity spectra at different wavelengths of near ultraviolet (NUV) region. On the other hand, the BND material for experimental method displays two peaks, which are in NUV region, while the BND material for theoretical method displays three peaks except for DCM solvent, which two of them are in NUV region and other is visible region. This figure shows us two important consequences. First, the absorbance and molar absorptivity spectra differ when different methods such as theoretical and experimental methods are used. Secondly, the absorbance and molar absorptivity spectra that differ in each method also vary with different solvents. Fig. 2b indicates the curves of photoluminescence (PL) intensity vs. λ of the BND material for various solvents. As seen in Fig. 2b, the BND displays the maximum peaks of the PL in the visible region and the positions of the PL are close to each other, but the maximum peak of the PL in chloroform is formed in a smaller wavelength. These results suggest that the BND material is suitable for photoluminescence devices.

4.3. Optical parameters of the BND solutions for different solvents

We obtained absorbance band edge E_{Abs-be}, mass extinction coefficient (α_{mass}), optical band gap (E_g) and refractive index (n) values of the BND solutions for DCM and chloroform solvents.

The E_{Abs-be} values of the BND solutions for DCM and chloroform solvents were achieved from the maximum peaks of the $dT/d\lambda$ curves vs. λ as seen in Fig. 3 and found to be about 3.29 and 3.31 eV, respectively. This result suggests that the absorbance band edge of the BND solution for DCM is lower than the absorbance band edge of the BND solution for chloroform.

The mass extinction coefficient of the BND in different solvents qualifies how easily it can be penetrated by a beam of light, particles, sound, or matter or other energy. With this term, the interaction of light and material is better understood. Thus, the response of these behaviors is of great importance for OLED applications. The α_{mass} coefficient depends on the molar extinction coefficient and is given by [44],

$$\alpha_{mass} = \frac{Abs}{CLM_A} \quad (1)$$

where C is the concentration of sample, L is the path length of the sample and M_A (322.36 g/mol for BND material) is the molecular weight. We calculated the α_{mass} values of the BND solutions in DCM and chloroform solvents from Eq. (1). The α_{mass} curves vs. photon energy (E) of the BND in DCM and chloroform is shown in Fig. 4. As seen in Fig. 4, the mass extinction coefficient values of the BND in DCM are higher than the mass extinction coefficient values of the BND in chloroform and the BND in DCM and chloroform exhibits the maximum peaks at about 5.28 and 5.12 eV, respectively. The maximum α_{mass} values of the BND solutions for DCM and chloroform solvents are 13.693 and 4.442 $Lg^{-1}\,cm^{-1}$, respectively.

The vital E_g parameter for optoelectronic applications can be obtained with Tauc model and is given the following equation [45],

$$\alpha(h\vartheta) = A(E-E_g)^m \quad (2)$$

where α is absorption coefficient, $h\vartheta$ and E are the photon energy, and A is a constant. For BND solutions, m was found as ½, which corresponds to allowed direct band gap. Thus, the $(\alpha h\vartheta)^2$ curves vs. E of the BND for DCM and chloroform were indicated in Fig. 5. To gain insight into photophysical behavior of all the studied solvents we analyzed energy gap values (see Table 1) of the BND organic molecule. By

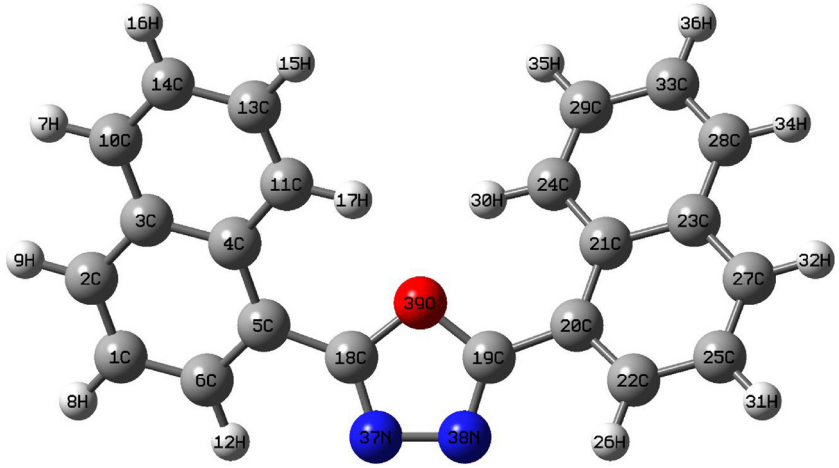

Fig. 1. Optimized ground state geometry of BND organic molecule with atom numbering calculated by B3LYP/6-311-G (d, p).

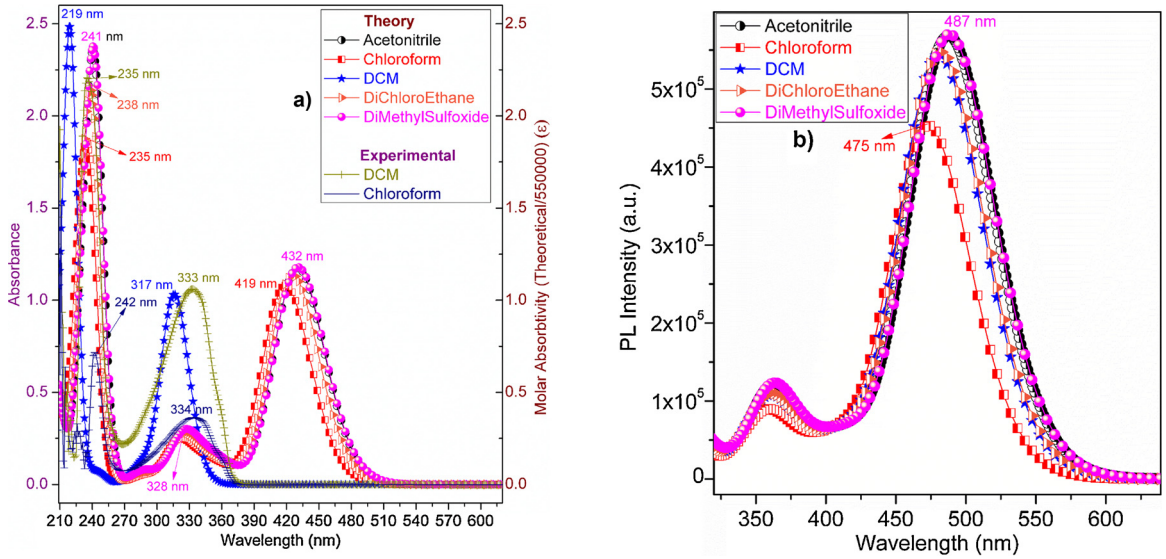

Fig. 2. a) The experimental and theoretical (for different solvents) molar absorptivity plots vs. wavelength (λ) b) PL intensity vs. wavelength of BND organic material.

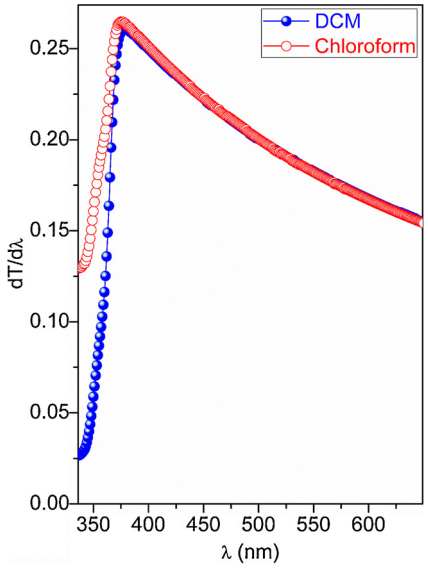

Fig. 3. (a) The $dT/d\lambda$ plot vs. wavelength (λ) of BND organic material for DCM and chloroform solvents.

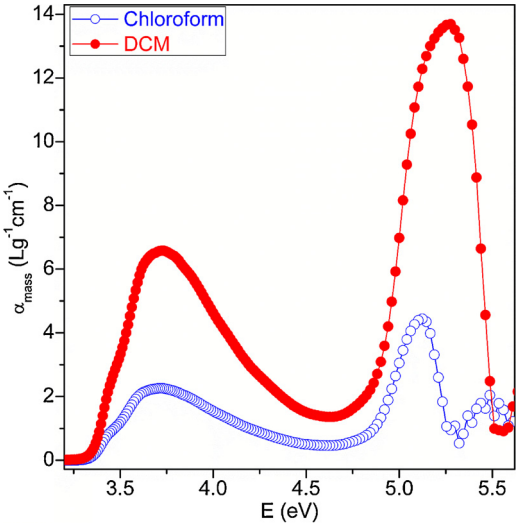

Fig. 4. The mass extinction coefficient (α_{mass}) plot vs photon energy (E) of BND organic material for DCM and chloroform solvents.

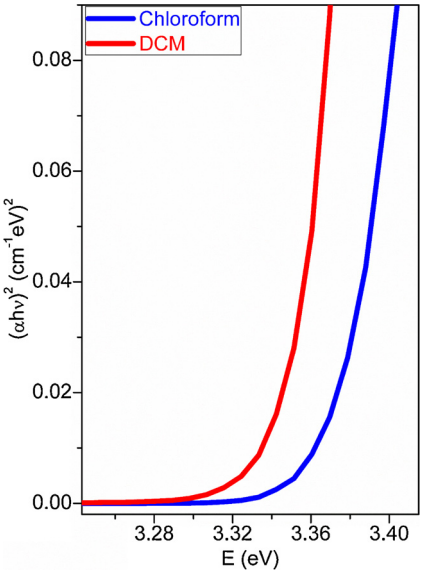

Fig. 5. The $(\alpha h\nu)^2$ vs photon energy (E) of BND organic solutions for different solvents.

Table 1
The refractive index values of the BND material obtained experimental optical band gap for DCM and chloroform solvents.

Solvents	Refractive index (n) values				
	Moss	Ravindra	Hervé-Vandamme	Reddy	Kumar-Singh
DCM	2,312	2,024	2,238	2,686	2,286
Chloroform	2,308	2,010	2,232	2,681	2,281

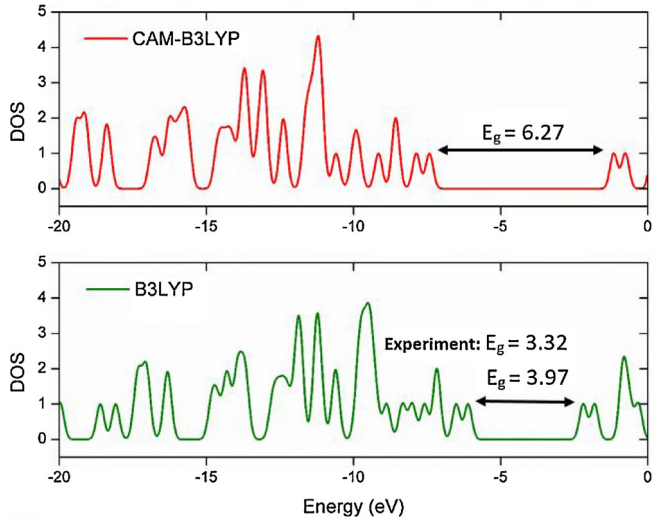

Fig. 6. Density of state (DOS) spectrum (for B3LYP and CAM-B3LYP functionals) of BND organic molecule in chloroform obtained from Mulliken population analysis.

extrapolating the linear plot to $(\alpha h\vartheta)^2 = 0$, we obtained the E_g values as 3.34 and 3.32 eV for DCM and chloroform. The energy gap increased by about 0.02 eV for the BND molecule in DCM solvent. The measured and calculated E_g results are also found to be consistent with the absorbance band edge results. We have also calculated HOMO, LUMO and E_g values using DFT approach with B3LYP (see Table 1) and CAM-B3LYP functionals (see Fig. 6). Comparing calculated E_g values with measured results, one can conclude that B3LYP (3.38 eV) gives better result than

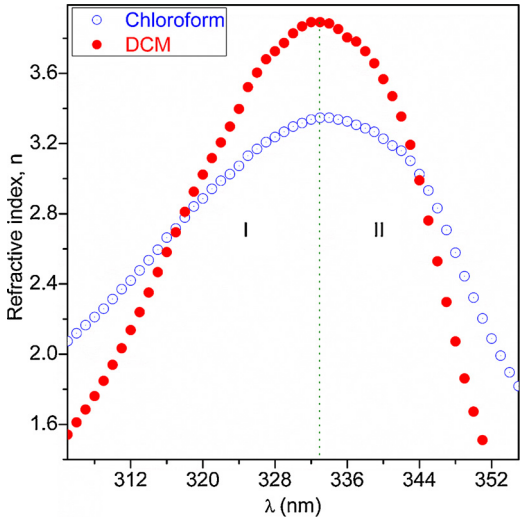

Fig. 7. The refractive index (n) curves wavelength (λ) of BND organic material for DCM and chloroform solvents.

that of CAM-B3LYP (6.27 eV). The lower optical band gap of the BND is obtained in DCE solvent comparing the other solvents DCM, DMS, acetonitrile and chloroform. The computational and experimental results indicate that the gap values of the BND change with the solvent environments. Comparing with DCE, DMS and acetonitrile solvents, the HOMO energy increased by about 0.1 eV in DCM while the LUMO energy level increased by about 0.04 eV. In addition, the derivatives of BND have considerable potential as multifunctional layers and as electron transport layers in OLED [25]. The HOMO and LUMO energy levels of the BND molecule in different solvent environments range from -2.17 to 2.21 eV and from -6.10 to -6.22 eV (see Table 1), indicating that BND organic molecule will function well as electron transport materials in OLED applications. From this viewpoint, the properties make the BND organic material suitable candidate for the preparation of OLEDs.

Another important optical parameter is the refractive index (n)parameter, which can be given using reflectance (R) by [46],

$$n = \left\{ \sqrt{\frac{4R}{(R-1)^2} - k^2} - \frac{R+1}{R-1} \right\} \tag{3}$$

Where $k = \alpha\lambda/4\pi$. We calculated the n values of BND for DCM and chloroform. Fig. 7 depicts the n curves vs. λ of the BND for DCM and chloroform. As seen in Fig. 7, the BND shows the normal (region I) and abnormal behavior (region II). These results suggest that the n values vary from about 1.6 to 3.9 in the NUV region. Then, we calculated the n values for various relations [47] such as Moss, Kumar-Singh, Ravindra, Hervé-Vandamme and Reddy. Obtained n values of the BND for DCM and chloroform are given in Table 2. As seen in Table 2, the lowest n values (2.024 and 2.010) of the BND for DCM and chloroform are obtained from Ravindra relation, while the highest n values (2.686 and

Table 2
The calculated HOMO and LUMO energies (eV) and energy gaps $(E_g, in\ eV)$ between HOMO and LUMO orbitals of BND organic molecule for different solvents. (Dichloromethane (DCM), dichloroethane (DCE), dimethyl sulfoxide (DMS), acetonitrile and chloroform).

Energy level (eV)	DFT/B3LYP/6–311 G (d, p)/(Experiment)				
	DCM	DCE	DMS	Acetonitrile	Chloroform
HOMO	6.22	6.10	6.12	6.12	6.19
LUMO	2.21	2.17	2.17	2.17	2.21
E_g	4.00/(3.34)	3.92	3.94	3.94	3.97/(3.32)

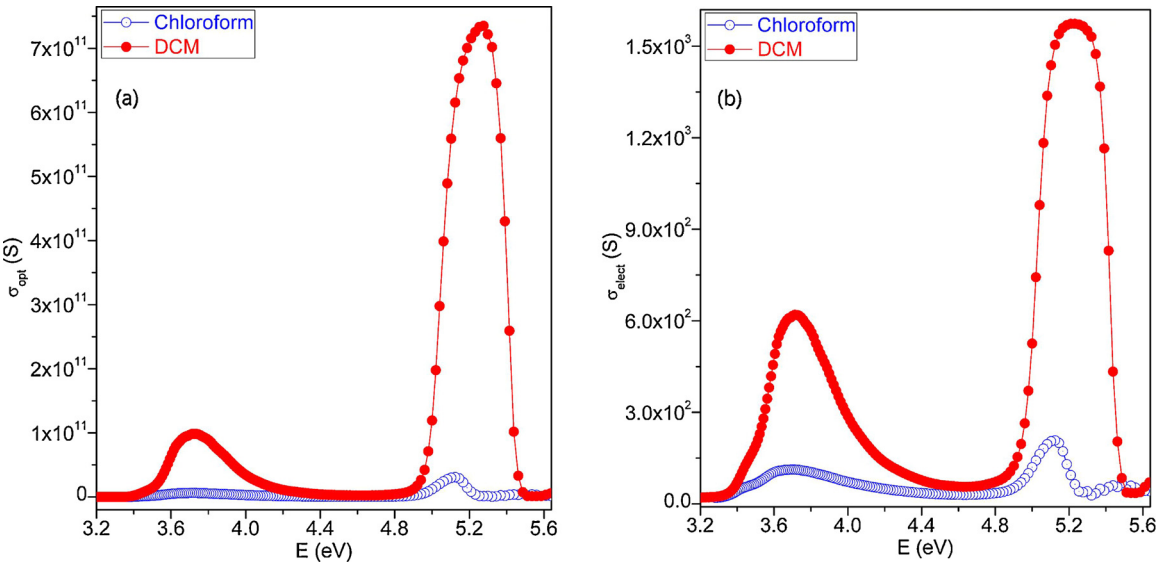

Fig. 8. (a) The optical conductance (σ_{opt}) and (b) electrical conductance (σ_{elect}) curves vs. (E) of BND organic material for DCM and chloroform solvents.

2.681) of the BND are obtained from Reddy relation. Also, the n values of the BND for DCM are slightly larger than the values of the BND for chloroform. This result shows that the BND material in DCM, which displays the lower optical band gap and higher refractive index can give the most results for OLED devices.

4.4. Conductance parameters of the BND solutions

The optical conductance (σ_{opt})and electrical conductance (σ_{elct})parameters are important for optical materials and devices [48,49]. σ_{opt} and σ_{elct} are given by [50], respectively.

$$\sigma_{opt} = \frac{\alpha nc}{4\pi} \tag{4}$$

and

$$\sigma_{elect} = \frac{2\lambda\sigma_{opt}}{\alpha} \tag{5}$$

where c is the speed of light. We obtained the σ_{opt} and σ_{elct} parameters of the BND for DCM and chloroform via Eqs. (4) and (5), respectively. The σ_{opt} and σ_{elct} curves vs. E of the BND for DCM and chloroform are shown in Fig. 8(a, b), respectively. As seen in Fig. 8(a), the optical conductance values of the BND for DCM and chloroform are in the range of 10^{11} and 10^{10} S, respectively. Also, the σ_{opt} values for DCM are higher than that of the σ_{opt} for chloroform. The highest optical conductance peak of the BND for DCM is observed at 5.277 eV. As seen in Fig. 8(b), the electrical conductance values of the BND for DCM and chloroform are in the range of 10^3 and 10^2 S, respectively. These results suggest that the optical and electrical conductance can be changed with solvent environments. In addition, the BND material in DCM, which exhibits the higher optical and electrical conductance can give the most results for OLED devices. We also observed this compatible result for the optical band gap and refractive indices obtained.

4.5. Mulliken atomic charges and dipole moments

The Mulliken atomic charges result from the Mulliken population analysis. The charges of BND organic molecule were given in Table 3. The charges in the different positions for of the same atoms show different characteristic properties. For example, C1, C2, C3 atoms exhibit a negative charge, however; C4 and C5 atoms show a positive charge (see Table 3). When it comes to DCM and chloroform solvents, the charge for DCM is bigger than that of chloroform. Hydrogen atom also exhibits a positive charge because it is an acceptor atom.

Table 3
Mullkien atomic charges (MACs) of BND for [a]Chloroform and [b]DCM solvents.

Atoms	[a]MACs	[b]MACs	Atoms	[a]MACs	[b]MACs
C1	−0.641999	−0.648523	C20	0.925658	0.922276
C2	−0.010335	−0.012887	C21	0.489725	0.490285
C3	−0.051861	−0.055240	C22	−0.311956	−0.312205
C4	0.489862	0.490424	C23	−0.051716	−0.055096
C5	0.925545	0.922164	C24	−0.476049	−0.475770
C6	−0.312231	−0.312478	C25	−0.642080	−0.648606
H7	0.163393	0.168607	H26	0.213485	0.213444
H8	0.198653	0.202799	C27	−0.010349	−0.012900
H9	0.163121	0.168603	C28	−0.383367	−0.383741
C10	−0.383436	−0.383812	C29	−0.403708	−0.409140
C11	−0.476084	−0.475804	H30	0.125031	0.127606
H12	0.213493	0.213450	H31	0.198651	0.202797
C13	−0.403548	−0.408981	H32	0.163121	0.168603
C14	−0.281802	−0.286826	C33	−0.281844	−0.286867
H15	0.194325	0.198118	H34	0.163396	0.168610
H16	0.184766	0.188956	H35	0.194323	0.198116
H17	0.125027	0.127600	H36	0.184767	0.188957
C18	−0.093357	−0.083003	N37	−0.034174	−0.045492
C19	−0.093151	−0.082795	N38	−0.034109	−0.045425
			O39	0.060814	0.064176

The dipole moments result from differences in electronegativity. When dipole moment is bigger stronger intermolecular interaction occur. The bigger value of the component of dipole moment along the y-axis (μ_y = 5.20 Debye) predicts large charge separation. The corresponding total dipole moment has been calculated to be about 5.20 Debye. The value of dipole moment of BND in DMS solvent is higher than that of DCM (5.14 Debye), DCE (4.98 Debye), acetonitrile (5.18 Debye) and chloroform (4.91 Debye) solvents.

4.6. Radial distribution function

The radial distribution functions (RDFs) give the probability of finding a particle in the distance from another particle. In this study, the purpose of the RDF is to compare experimental theoretical RDF results. The theoretical RDF is found to be in good agreement with the results of the theoretical study. From Fig. 9, one can see that calculated RDF is greater than that of measured. Both calculated and measured values are greater in the range of 1–1.5 Å. Theoretical RDF result is greater than the experimental one in this range. It also has a narrower distribution than experimental distributions.

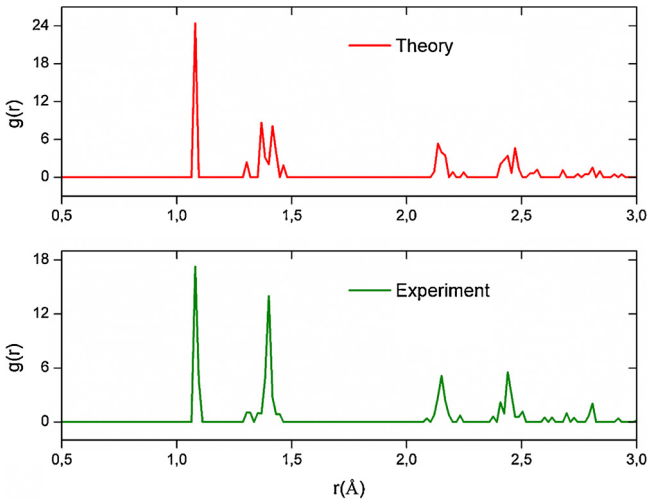

Fig. 9. The radial distribution functions (RDFs) of BND organic molecule obtained from theory and experiment.

5. Conclusions

Based on the experimental and theoretical techniques, photophysical, electronic structure and spectroscopic properties of BND organic material have been investigated. From the results, the optimized structure with minimum total energy is the C_1 form. Predicted band energy values using B3LYP functional give better results than that of CAM-B3LYP, comparing with experimental data, however; calculated molar extinction coefficients using CAM-B3LYP functional gives reasonable results than that of B3LYP. From the lowest vibrational frequencies and the energy gap results, the compound in DCM is more stable than that of chloroform solvent. Radial distribution functions (RDFs) were also recorded using DFT and experimental results. Optical band gaps and refractive indices of the molecule were controlled with different solvents. Moreover, DCM solvent can be preferred for optical devices with lower absorbance band edge, lower optical band gap, and higher mass extinction coefficient, higher optical and electrical conductance. These differences are also due to solvatochromism of the solvents with different polarities. Because the solvents change the position and shape of the material and thus the density of the absorption band.

Acknowledgments

The numerical calculations reported in this paper were partially performed at TUBITAK ULAKBIM, High Performance and Grid Computing Centre (TRUBA resources), Turkey. This work was supported by the Ahi Evran University Scientific Research Projects Coordination Unit. Project Number: PYO-FEN.4001.14.009.

References

[1] S. Reineke, F. Linder, G. Schwartz, N. Seidler, K. Walazer, B. Lüssem, K. Leo, Nature 459 (2009) 234.
[2] F. So, J. Kido, P. Burrows, MRS Bull. 33 (2008) 663.
[3] T. Nakayama, K. Hiyama, K. Furukawa, H. Ohtani, SID 16 (2008) 231.
[4] J. Chen, F. Zhao, D. Ma, Mater. Today 17 (2014) 175.
[5] J. Lee, W.J. Sung, C.W. Joo, H. Cho, N.S. Cho, G.-W. Lee, D.-H. Hwang, J.-I. Lee, ETRIJ 38 (2016) 260.
[6] F. Wudl, G. Srdanov, US Patent 5189136, 1993.
[7] A. Ltaief, A. Bouazizi, J. Davenas, R. Ben Chaabane, H. Ben Ouada, Synth. Met. 147 (2004) 261.
[8] F.-M. Hsu, C.-H. Chien, P.-I. Shih, C.-F. Shu, Chem. Mater. 21 (2009) 1017.
[9] K.T. Kamtekar, A.P. Monkman, M.R. Bryce, Adv. Mater. 22 (2010) 572.
[10] B. Zhang, G. Tan, C.S. Lam, B. Yao, C.L. Ho, L. Liu, Z. Xie, W.Y. Wong, J. Ding, L. Wang, Adv. Mater. 24 (2012) 1873.
[11] Z. Yu, X. Niu, Z. Liu, Q. Pei, Adv. Mater. 23 (2011) 3989.
[12] S. Reineke, F. Lindner, G. Schwartz, N. Seidler, K. Walzer, B. Lussem, K. Leo, Nature 459 (2009) 234.
[13] Y. Sun, N.C. Giebink, H. Kanno, B. Ma, M.E. Thompson, S.R. Forrest, Nature 440 (2006) 908.
[14] M. Kurban, B. Gündüz, J. Mol. Struct. 1137 (2017) 403.
[15] J. Zhao, X. Chen, Z. Yang, Z. Chi, Z. Yang, Y. Zhang, J. Xu, Z. Chi, M.P. Aldred, J. Mater. Chem. C 6 (2018) 3226.
[16] T.-H. Han, M.-R. Choi, C.-W. Jeon, Y.-H. Kim, S.-K. Kwon, T.-W. Lee, Sci. Adv. 2 (2016) e1601428.
[17] P. Bujak, I.K.- Bajer, Zagorska M, V. Maurel, I. Wielgus, A. Pron, Chem. Soc. Rev. 42 (2013) 8895.
[18] G.S. He, L.-S. Tan, Q. Zheng, P.N. Prasad, Chem. Rev. 108 (2008) 1245.
[19] H. Tokuhisa, M. Era, T. Tsutsui, S. Saito, Appl. Phys. Lett. 66 (1995) 3433.
[20] J. Preston, J. Heterocycl. Chem. 2 (1965) 441.
[21] C.-H. Chang, R. Griniene, Y.-D. Su, C.-C. Yeh, H.-C. Kao, J.V. Grazulevicius, et al., Dyes Pigm. 122 (2015) 257.
[22] M. Reig, C. Gozalvez, R. Bujaldon, G. Bagdziunas, K. Ivaniuk, N. Kostiv, et al., Dyes Pigm. 137 (2017) 24.
[23] Z. Peng, Z. Bao, M.E. Galvin, Adv. Mater. 10 (1998) 680.
[24] X. Yang, X. Xu, G. Zhou, J. Mater. Chem. C 3 (2015) 913.
[25] Y. Tao, C. Yang, J. Qin, Chem. Soc. Rev. 40 (2011) 2943.
[26] G. Hughes, M.R. Bryce, J. Mater. Chem. 15 (2005) 94.
[27] H. Tokuhisa, M. Era, T. Tsutsui, Synth. Met. 85 (1997) 1161-l–162.
[28] M.A. Reddya, G. Malleshama, A. Thomas, K. Srinivas, V. Jayathirtha Rao, K. Bhanuprakash, L. Giribabu, R. Grover, A. Kumar, M.N. Kamalasanan, R. Srivastava, Synth. Met. 161 (2011) 869.
[29] K. Krukiewicz, T. Jarosz, A.P. Herman, R. Turczyn, S. Boncel, J.K. Zak, Synth. Met. 217 (2016) 231.
[30] H. Yu, Synth. Met. 160 (2010) 2505.
[31] B. CheolJeon, M. SeokKim, M. JuCho, D.H. Choi, K.-S. Ahn, J.H. Kim, Synth. Met. 188 (2014) 130.
[32] B. Gündüz, M. Kurban, Vib. Spectrosc. 96 (2018) 46.
[33] Y. Liu, H.C. Du, G. Wang, et al., Int. J. Quant. Chem. 111 (2011) 1115.
[34] W. Kohn, L.J. Sham, Phys. Rev. 140 (1965) A1133.
[35] A.D. Becke, Phys. Rev. A 38 (1988) 3098.
[36] S.H. Vosko, L. Vilk, M. Nusair, Can. J. Phys. 58 (1980) 1200.
[37] C. Lee, W. Yang, R.G. Parr, Phys. Rev. B 37 (1988) 785.
[38] T. Yanai, D.P. Tew, N.C. Handy, Chem. Phys. Lett. 393 (2004) 51.
[39] M.E. Foster, B.M. Wong, J. Chem. Theory Comput. 8 (2012) 2682.
[40] A.P. Basile, F.E. Curchod, A. Fabrizio, L. Floryan, C. Corminboeuf, J. Phys. Chem. Lett. 6 (1) (2015) 13.
[41] İ. Muz, M. Kurban, Inorganica Chim. Acta 477 (2018) 318.
[42] M. Kurban, B. Gündüz, Optik 165 (2018) 370.
[43] M.J. Frisch, G.W. Trucks, H.B. Schlegel, G.E. Scuseria, M.A. Robb, J.R. Cheeseman, G. Scalmani, V. Barone, B. Mennucci, G.A. Petersson, et al., Gaussian 09, Revision B.01, Gaussian, Inc., Wallingford CT, 2009.
[44] A. Beer, Ann. Phys. 86 (1852) 78.
[45] J. Tauc, A. Menth, J. Non-Cryst. Solids 569 (1972) 8.
[46] F. Abeles, Optical properties of solids. North-Holland Publishing Company, London, Amsterdam.
[47] S.K. Tripathy, Opt. Mater. 46 (2015) 240.
[48] M. Yarmohammadi, AIP Adv. 6 (2016) 085008.
[49] M. Kurban, B. Gündüz, Chem. Phys. Lett. 691 (2018) 14.
[50] J.O. Akinlami, I.O. Olateju, Semicond. Phys. Quantum Electron. 153 (2012) 281.